Environmental Science & Technology

Article

pubs.acs.org/est

Effect of Dissolved Organic Matter Source and Character on Microbial Hg Methylation in Hg−S−DOM Solutions

Andrew M. Graham,*[,†,‡] George R. Aiken,[§] and Cynthia C. Gilmour[‡]

[†]Department of Chemistry, Grinnell College, Noyce Science Center, 1116 Eighth Avenue, Grinnell, Iowa 50112-1690, United States

[‡]Smithsonian Environmental Research Center, P.O. Box 28, Edgewater, Maryland 21037, United States

[§]U.S. Geological Survey, 3215 Marine Street, Suite E127, Boulder, Colorado 80303, United States

Supporting Information

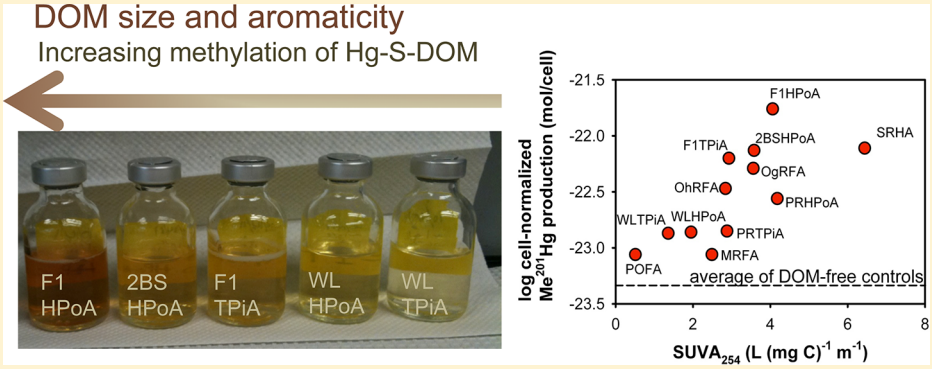

ABSTRACT: Dissolved organic matter (DOM) is a key component of fate and transport models for most metals, including mercury (Hg). Utilizing a suite of diverse DOM isolates, we demonstrated that DOM character, in addition to concentration, influences inorganic Hg ($Hg(II)_i$) bioavailability to Hg-methylating bacteria. Using a model Hg-methylating bacterium, *Desulfovibrio desulfuricans* ND132, we evaluated Hg-DOM-sulfide bioavailability in washed-cell assays at environmentally relevant Hg/DOM ratios (~1−8 ng Hg/mg C) and sulfide concentrations (1−1000 μM). All tested DOM isolates significantly enhanced Hg methylation above DOM-free controls (from ~2 to >20-fold for 20 mg C/L DOM solutions), but high molecular weight/highly aromatic DOM isolates and/or those with high sulfur content were particularly effective at enhancing Hg methylation. Because these experiments were conducted under conditions of predicted supersaturation with respect to metacinnabar (β-HgS(s)), we attribute the DOM-dependent enhancement of $Hg(II)_i$ bioavailability to steric and specific chemical (e.g., DOM thiols) inhibition of β-HgS(s) growth and aggregation by DOM. Experiments examining the role of DOM across a wide sulfide gradient revealed that DOM only enhances Hg methylation under fairly low sulfide conditions ($\lesssim$30 μM), conditions that favor HgS nanoparticle/cluster formation relative to dissolved HgS species.

INTRODUCTION

Dissolved organic matter (DOM) plays a central role in the biogeochemical cycling of mercury. Processes affected by DOM include inorganic mercury ($Hg(II)_i$) complexation[1−5] and transport,[6,7] methylmercury (MeHg) complexation[8,9] and transport,[7,10] precipitation[11−14] and dissolution[13,15,16] of Hg−S minerals, and MeHg production by bacteria.[17,18] Understanding factors that influence MeHg production is paramount for risk evaluation and management in Hg-impacted ecosystems, as microbial Hg production is the main driver of risk associated with Hg pollution.

MeHg production occurs mainly in anoxic soils and sediments[19−21] where dissolved, nanoparticulate, and particulate Hg−sulfide species are often the predominant forms of $Hg(II)_i$.[12,14,21−23] Previously, we demonstrated that DOM can strongly enhance the bioavailability of $Hg(II)_i$ to a Hg-methylating sulfate-reducing bacterium under conditions typical of mildly sulfidic anoxic sediment or soil porewaters.[18] We attributed this novel finding to the role that DOM plays in stabilizing metal sulfide nanoparticles against growth and aggregation,[11,12,14,24] and hypothesized that sufficiently small and/or disordered forms of HgS might be bioavailable to Hg-methylating bacteria. Parallel work by Zhang et al.[25] supports this hypothesis by confirming that nanoscale metacinnabar (β-HgS(s)) is more bioavailable to Hg-methylating bacteria than bulk β-HgS(s).

In this study, we evaluate the effect of DOM source and character on microbial methylation rates in Hg-DOM-sulfide solutions, using a model Hg-methylating bacterium, *Desulfovibrio desulfuricans* ND132. Twelve DOM isolates, originating from a variety of lacustrine, riverine, wetland, and marine

Received: January 27, 2013
Revised: May 1, 2013
Accepted: May 1, 2013
Published: May 1, 2013

Table 1. Characteristics of DOM Isolates Used in This Study

isolate	site description	C (%)	H (%)	O (%)	N (%)	S (%)	Ash (%)	$SUVA_{254}$ (L (mg C)$^{-1}$ m^{-1})
FL Everglades site 2BS hydrophobic acid (2BSHPoA)	Marshland in Water Conservation Area 2BS in FL Everglades	52.3	4.8	40.2	1.6	1.2	7.3	3.58 ± 0.05
FL Everglades site F1 hydrophobic acid (F1HPoA)	Eutrophied marshland in Water Conservation Area 2A in FL Everglades	52.7	4.8	39.2	1.7	1.6	2.8	4.06 ± 0.06
FL Everglades site F1 transphilic acid (F1TPiA)	Eutrophied marshland in Water Conservation Area 2A in FL Everglades	48.0	4.6	43.1	2.7	1.5	4.2	2.93 ± 0.04
Missouri River fulvic acid (MRFA)	Major river draining north-central US, sampled at Sioux City, IA	56.7	5.4	35.8	1.3	0.8	0.1	2.49 ± 0.04
Ogeechee River fulvic acid (OgRFA)	Small river draining Piedmont of eastern Georgia, sampled at Grange, GA	54.3	4.8	38.6	0.9	1.3	0.4	3.56 ± 0.07
Ohio River fulvic acid (OhRFA)	Major river draining east-central US, sampled at Cincinnati, OH	55.8	5.4	36.0	1.5	1.3	0.6	2.84 ± 0.07
Pacific Ocean fulvic acid (POFA)	Sample collected from 100 m depth 170 km southwest of Honolulu, HI	56.2	6.0	36.3	1.1	0.4	0.4	0.51 ± 0.03
Penobscot River hydrophobic acid (PRHPoA)	River draining central Maine, sampled at Eddington, Maine	52.7	4.3	41.4	1.1	0.5	4.0	4.18 ± 0.08
Penobscot River transphilic acid (PRTPiA)	River draining central Maine, sampled at Eddington, Maine	47.1	4.2	47.0	1.7	n.d.[a]	9.5	2.88 ± 0.03
Suwannee River humic acid (SRHA, Standard II)	Blackwater river draining Okeefenokee Swamp, sampled at Fargo, GA	52.6[b]	4.3[b]	42.0[b]	1.2[b]	0.5[b]	1.04[b]	6.44 ± 0.15
Williams Lake hydrophobic acid (WLHPoA)	Seepage lake in north-central Minnesota	55.2	5.7	36.5	1.8	0.8	2.1	1.95 ± 0.02
Williams Lake transphilic acid (WLTPiA)	Seepage lake in north-central Minnesota	49.6	5.4	40.6	3.4	1.0	1.9	1.36 ± 0.02

[a]n.d. = not determined due to insufficient material. [b]Data provided by International Humic Substances Society (IHSS).

environments, were evaluated for their impact on Hg-methylation rates at environmentally relevant Hg/DOM ratios (~0.025 nmol/mg C) and sulfide concentrations (~1−1000 μM). Several field studies have shown that DOM character, particularly specific UV absorbance (SUVA; a measure correlated to the size and aromaticity of DOM[26]), is a strong correlate of net MeHg production.[27,28] Laboratory studies have conclusively demonstrated that DOM size and aromaticity are strongly linked to Hg−S dissolution,[16] precipitation/aggregation,[29] and ordering of HgS.[29] In this paper we describe carefully controlled experiments designed to test the hypothesis that DOM character (especially DOM size and aromaticity) is a significant driver of Hg−S bioavailability to Hg-methylating bacteria. Our results have implications for predicting MeHg production rates in natural systems. They are particularly relevant to predicting the impacts of ecosystem-level perturbations that affect the concentration and quality of DOM (e.g., land use change and alteration of surface/subsurface hydrology,[30,31] eutrophication,[31] postacidification recovery,[32,33] etc.).

EXPERIMENTAL SECTION

DOM Isolation and Characterization. DOM fractions were isolated from a variety of ecosystem types encompassing a wide range of trophic states and organic matter sources (Table 1). Suwannee River humic acid (SRHA, Standard II) was obtained from the International Humic Substances Society (IHSS) and used without additional purification; all other DOM samples were isolated according to methods described previously.[34,35] For each DOM isolate, the elemental composition of the freeze-dried isolate was determined by Huffman Laboratories (Golden, CO). Specific UV absorbance at λ = 254 nm ($SUVA_{254}$) for each isolate was measured by preparing ~10 mg C/L stocks of each DOM isolate, filtering through 0.2 μm filters, and measuring total dissolved organic carbon with a Shimadzu TOC-V_{CSH} total organic carbon analyzer and UV absorbance at λ = 254 nm with a Cary 4E UV−vis spectrophotometer. Additional information (average molecular weight, ^{13}C NMR, and sulfur speciation by X-ray near edge absorption spectroscopy (XANES)) has been previously compiled for a subset of these samples.[16]

Cell Cultivation and Maintenance. *Desulfovibrio desulfuricans* ND132 was employed as a model Hg-methylating sulfate reducing bacterium (SRB). Strain ND132 was isolated from Chesapeake Bay bottom sediments.[36] It is well characterized with respect to its growth[37] and Hg-methylation capability (including in Hg-DOM-sulfide solutions)[18,37,38] and has a fully sequenced genome.[39] Strain ND132 was maintained on estuarine pyruvate-fumarate (EPF) growth medium, which supports respiratory growth with sulfide production limited to that produced via L-cysteine degradation.[18]

Impact of DOM Character on MeHg Production. We evaluated the effect of DOM source and character on MeHg production by strain ND132 in carefully controlled washed cell assays.[38] Cells were grown to midlog phase (optical density at λ = 660 nm of ~0.2), harvested by centrifugation (3000× *g*), and resuspended in EPF wash buffer (recipe given in Graham et al.[18]). Cell suspensions were then centrifuged a second time (3000× *g*) and the cell pellet was resuspended in EPF assay buffer. The assay buffer consisted of the basic EPF wash buffer amended with 20 mg C/L of DOM isolate (see Table 1; added from TOC-measured ~500 mg C/L freshly prepared, 0.2 μm-filtered stocks made in N_2-purged deionized water) and 0.5 nM of stable-isotope enriched $^{201}HgCl_2$ (98.11% enriched in ^{201}Hg, Oak Ridge National Laboratories, Oak Ridge, TN). Filter-sterilized assay buffer was equilibrated for 24 h at 31 °C in the dark prior to resuspension of the ND132 cells. Cell suspensions were incubated in the dark for 3 h at 31 °C, and MeHg production as well as total Hg (THg) partitioning were measured at the end of the incubation period. Washed cell assays were performed in triplicate for each DOM isolate. All sample manipulations were performed under strictly anoxic

conditions inside a glovebag (Coy Laboratory Products, Grass Lake, MI) with a 95% N_2, 5% H_2 atmosphere and Pd catalyst for O_2 removal. The enriched stable isotope approach was necessary to separate the Hg spike from Hg found in the DOM isolates or other medium components.

Each experimental set included triplicate no-DOM controls and triplicate positive controls containing 500 μM L-cysteine without DOM addition. The 500 μM L-cysteine positive controls allow us to measure Hg methylation efficiency of $Hg(II)_i$ in a highly bioavailable form.[40] These cysteine controls can then be used to assess and correct for differences in methylation efficiencies across experiments conducted on different days with cells harvested at slightly different cell densities. Our previous work indicated that abiotic Hg methylation by DOM was insignificant.[18] Low sulfide concentrations (generally 1.0−2.0 μM) in the assays were obtained from ND132's degradation of L-cysteine provided in the growth medium prior to cell washing.

At the onset of each 3 h methylation assay, we measured optical density (OD_{660}), cell density, total cell protein, pH, and inorganic sulfide. At the end of the incubation, we removed aliquots for OD_{660}, total cell protein, pH, sulfide, total MeHg and THg, filter-passing (0.2 μm polycarbonate track etched filters (Whatman)) MeHg and THg, and particulate MeHg and THg (MeHg or THg retained on the filter). MeHg and THg samples were preserved by acidifying with 0.5% v/v trace metal grade HCl and stored frozen until analysis. To close mass balance on THg, filter flasks containing assay buffer were directly amended with 0.5% v/v trace metal grade HCl and 3% v/v BrCl to recover any Hg adsorbed to bottle walls during the 24 h pre-equilibration period.

Effect of Sulfide Concentration on Hg-DOM-S Bioavailability. The bioavailability of $Hg(II)_i$ in Hg-DOM-sulfide solutions was also evaluated over a much wider range of sulfide concentrations. These experiments were conducted as described above except that ∼3−1000 μM sulfide was added to the assay buffer 1−2 h prior to challenging ND132. In these experiments, the assay buffer consisted of the base EPF wash buffer, 0 or 20 mg C/L of SRHA, 1 nM $^{201}HgCl_2$, and various concentrations of sulfide. Each experiment included samples unamended with sulfide (with and without DOM addition) and positive controls without sulfide addition but with 500 μM L-cysteine addition. Treatments were repeated in duplicate for three of the six different sulfide spike concentrations for each experimental set (with and without DOM).

Analytical Methods. Cell density was measured with a Coulter Counter (Beckman Coulter Multisizer 4, Brea, CA). Samples for cell counting were diluted in ISOTON II electrolyte (Beckman Coulter) and analyzed by counting 50 μL volumes using a 20 μm aperture tube (calibrated against National Institute of Standards and Technology (NIST) certified latex beads with nominal diameter of 2 μm). Sulfide analyses were accomplished by diluting samples in sulfide antioxidant buffer (SAOB) and measuring the potential of diluted samples with a sulfide specific electrode (calibrated against Pb titrated Na_2S standards).[41] Samples for total cell protein were stored frozen until analysis and then analyzed via the Bradford protein assay.[42]

MeHg was determined by isotope dilution (ID) gas chromatography (GC) inductively coupled plasma mass spectrometry (ICP-MS) following aqueous phase distillation and ethylation.[28,43] Stable isotope enriched $Me^{199}Hg$ was synthesized in-house via reaction of $^{199}HgCl_2$ (Oak Ridge National Laboratories, 91.95% enriched in ^{199}Hg) with methylcobalamin,[44] and was used as the ID spike. MeHg concentrations of ambient and tracer ($Me^{201}Hg$) were calculated based on isotope abundances after correcting for impurities in the ID spike and ^{201}Hg tracer.[43] All MeHg measurements were made using a Brooks Rand MERX automated MeHg system (Seattle, WA) interfaced to a Perkin-Elmer Elan DRC II ICP-MS (Shelton, CT).

Total Hg (THg) was determined on digested samples by $SnCl_2$ reduction and detection of Hg(0) vapor with flow injection ICP-MS.[28] Total Hg in medium (unfiltered samples) and particulate THg (on filters) samples were digested in hot 7:4 v/v HNO_3/H_2SO_4 (1:2 v/v sample digest acid) until vapors turned colorless and were then preserved with 1% v/v BrCl. Filter-passing THg samples were digested overnight with 1% v/v BrCl at room temperature. Concentrations of excess ^{201}THg were calculated based on isotope abundances after correcting for impurities in the isotope tracer.[43] A summary of relevant QA/QC information for MeHg and THg analyses can be found in the Supporting Information.

RESULTS AND DISCUSSION

Hg Methylation and Hg Partitioning. All tested DOM isolates enhanced Hg methylation relative to DOM-free controls (Figure 1). Enhancement ranged from ∼2 to ∼22-fold on a percent methylation basis. For each DOM isolate and control, we tracked Hg and MeHg partitioning behavior. In all experimental treatments, 0.1 to 0.3 nM (roughly 20 to 65%) of added ^{201}THg was lost to bottle walls during the 24 h pre-equilibration period prior to challenging ND132. Total ^{201}Hg recovery following HCl/BrCl addition directly to pre-equilibration vessels was 92.5 ± 18.2%, indicating that losses due to Hg(II) reduction and Hg^0 evasion were minimal. Some isolates were more effective at limiting THg sorption to bottle walls than others, but differences in THg partitioning were not the major drivers of differences in Hg methylation. Total $Me^{201}Hg$ production was not correlated with either total ^{201}THg ($p = 0.1$, $r^2 = 0.07$) or filter-passing ^{201}THg ($p = 0.8$, $r^2 < 0.01$). We observed a statistically significant ($p < 0.05$; one-way ANOVA) enhancement for all DOM additions (compared to DOM-free controls) regardless of whether data were compared as total $Me^{201}Hg$ production, $Me^{201}Hg$ production normalized to cell density, or percent ^{201}Hg methylation (total $Me^{201}Hg$/total ^{201}THg in medium). Other potential experimental variables (pH, sulfide concentration, and cell density) were held approximately constant within a given experimental set (see Supporting Information Table S1) and could not account for the differences in Hg-methylation across DOM isolates.

Within each set of methylation assays, we included a positive control containing 500 μM L-cysteine. As noted previously,[18,40,45] Hg(II) is highly bioavailable in the presence of cysteine. We observed 87 ± 3% and 64 ± 5% of total ^{201}Hg methylated, respectively, in the two positive control experiments with cysteine. Percent ^{201}Hg methylation in treatments with 20 mg C/L DOM was lower and ranged from 2.7 to 32%. DOM-free controls yielded the lowest percent ^{201}Hg methylated, with 2.1 ± 0.1% and 0.88 ± 0.02% of measured ^{201}THg methylated in two DOM-free control assays. The difference in % Hg methylation in the control (500 μM cysteine addition and DOM-free) experiments conducted at different times likely reflects differences in cell density and/or cell

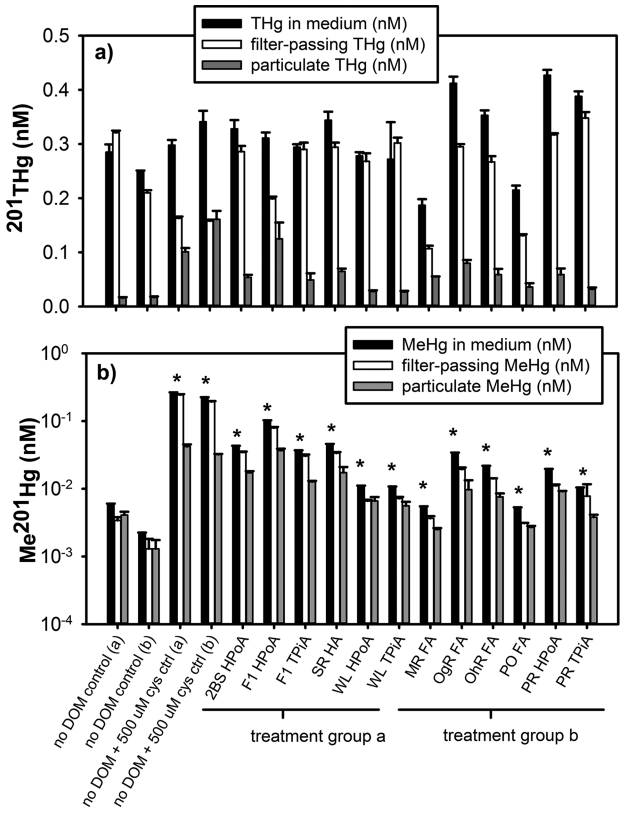

Figure 1. Effect of DOM isolate addition on (a) Hg partitioning and (b) MeHg production (note log scale) by *Desulfovibrio desulfuricans* ND132. Cells were incubated at 31 °C for 3 h in media containing 0.5 nM $^{201}HgCl_2$ pre-equilibrated with 20 mg C/L of each DOM isolate for 24 h. Experiments were performed in two batches (treatment groups a and b), each with a no DOM control and a positive control without DOM amended with 500 μM L-cysteine. Error bars show standard deviations of triplicate methylation assays. Bars in (b) with asterisk indicate total MeHg significantly greater than DOM-free controls ($p < 0.001$).

growth stage at the time of cell harvesting. MeHg production in the control experiments can serve as a normalization factor that allows for comparison of data for methylation assays with small differences in cell density and/or growth stage.

The majority of produced $Me^{201}Hg$ was exported from cells during the 3 h assays (Figure 1b). Across all of the experiments (including DOM-free controls and cysteine containing positive controls), filter-passing $Me^{201}Hg$ represented 70.7 ± 12.7% of the total $Me^{201}Hg$ measured at the end of the experiment. MeHg export in the cysteine-containing positive controls was 90.6 ± 3.5% of total MeHg production but only 58.4 ± 1.0% in DOM-free, cysteine-free controls. The average of 70% MeHg export is similar to that reported in our earlier work across DOM concentration gradients[18] or with various *Desulfovibrio* species.[38] Interestingly, with this larger data set looking at Hg methylation in the presence of a variety of DOM isolates, we did observe a positive correlation between total $Me^{201}Hg$ production and the fraction of $Me^{201}Hg$ that was filter (0.2 μm) − passing ($r^2 = 0.53$, $p < 0.001$). This correlation implies that factors that enhance $Hg(II)_i$ bioavailability for uptake and methylation may also enhance the extracellular export of MeHg.

Influence of DOM Character on Hg−S−DOM Methylation. All of the DOM isolates that we evaluated were found to significantly enhance $Me^{201}Hg$ production under mildly sulfidic conditions, but the degree of enhancement varied substantially depending on the identity of the DOM isolate. In order to help understand the DOM properties that influence bioavailability in Hg-DOM-S solutions, we performed regression analyses examining the relationships between various DOM characteristics and MeHg production in the short term washed cell assays. MeHg data were log transformed to achieve normality before regression analysis.

Significant positive correlations with MeHg production were observed for $SUVA_{254}$ ($r^2 = 0.51$, $p = 0.009$ for regression vs log cell-normalized $Me^{201}Hg$ and $r^2 = 0.41$, $p = 0.02$ for regression vs log $\%Me^{201}Hg$; Figure 2a and c) and organic matter sulfur content ($r^2 = 0.36$, $p = 0.05$ for log cell-normalized $Me^{201}Hg$; $r^2 = 0.42$, $p = 0.032$ for log % $Me^{201}Hg$; Figure 2b and d). No significant relationships were found between either N content or C/N ratio and MeHg production. Modeled together, $SUVA_{254}$ and S content explained 86% of the variability in MeHg production ($p < 0.001$).

$$\log[\text{cell} - \text{normalized}\, Me^{201}Hg] = -23.7 + 0.19 \times SUVA_{254} + 0.58 \times [S(wt\%)] \quad (1)$$

MeHg production in the Hg-DOM-S solutions was well described by the two-parameter model with the exception of the F1 HPoA isolate, for which the model under-predicted observed Hg methylation (Supporting Information Figure S1).

In our previous paper,[18] we hypothesized that DOM enhanced methylation primarily by limiting β-HgS(s) growth and/or aggregation[12−14] and that molecular clusters or nanoparticles of HgS were bioavailable to Hg-methylating bacteria. Concurrent work by Zhang et al.[25] clearly showed smaller, more poorly ordered HgS to be more bioactive, even after correcting for surface area effects. Our finding that $SUVA_{254}$ was correlated to $Hg(II)_i$ uptake/methylation is consistent with the idea that DOM sterically hinders HgS formation[11,12,14,24,29] and that smaller and/or poorly ordered species are more bioavailable to Hg methylating bacteria.[18,25] A growing body of literature indicates that DOM size and aromaticity are important controls on metal sulfide nanoparticle growth.[11,24] ZnS(s) growth rates determined by dynamic light scattering have been shown to negatively correlate with $SUVA_{280}$ (a metric linked to DOM size and aromaticity[26]). Using extended X-ray absorption fine structure (EXAFS), Gerbig[29] found that the Hg coordination number of metacinnabar-like nanoparticles decreased linearly with increasing $SUVA_{254}$.

We hypothesize that Hg methylation rates in Hg-DOM-sulfide solutions are correlated to $SUVA_{254}$ precisely because DOM properties (SUVA, molecular weight, aromaticity) that govern HgS particle growth profoundly influence $Hg(II)_i$ bioavailability and methylation. As a further test on this idea, we compared methylation in Hg-DOM-S solutions containing hydrophobic and transphilic acid fractions isolated from the same site. The hydrophobic acid fraction contains a greater proportion of aromatic C than does the transphilic fraction.[35] For two of the three isolate pairs (Florida Everglades F1 site and Penobscot River site), Hg-methylation was 2−3 fold higher for the hydrophobic acid fraction compared to the transphilic acid fraction (methylation rates for the Williams Lake isolates were statistically indistinguishable).

Field data corroborate our laboratory findings. MeHg concentrations in the field have been positively correlated

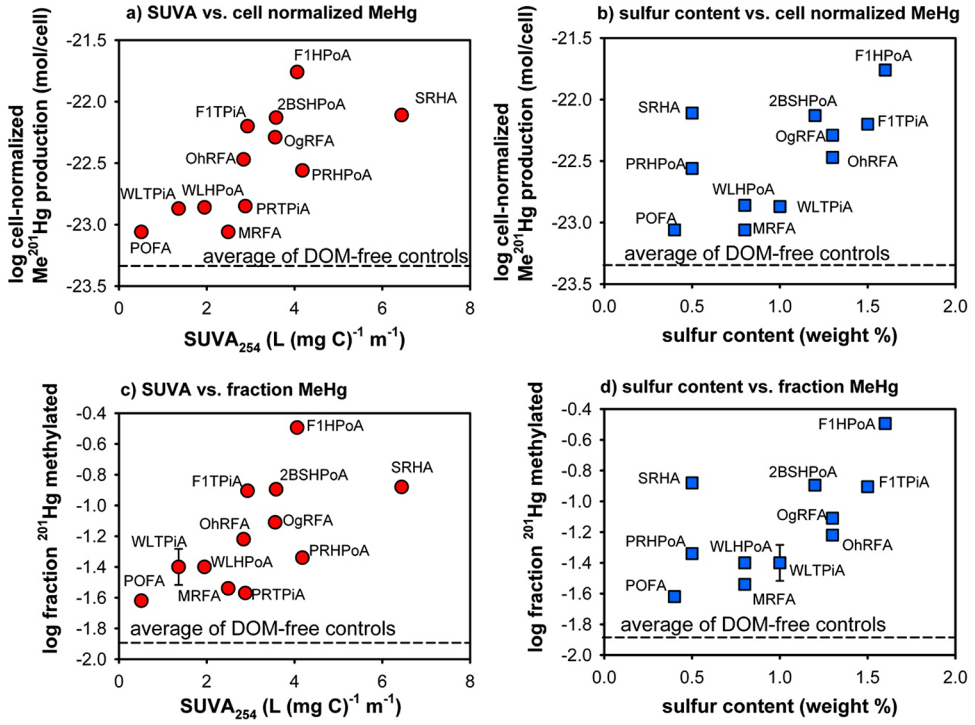

Figure 2. DOM properties influence MeHg production by strain ND132 in short-term washed cell assays containing 0.5 nM added $^{201}HgCl_2$, 20 mg C/L of each DOM isolate, and 1.5 ± 0.2 μM H_2S_T. Panels (a) and (b) show the relationship between cell normalized MeHg production and specific UV absorbance at 254 nm ($SUVA_{254}$) and sulfur content of DOM isolate, respectively. Panels (c) and (d) show relationships between fractional MeHg production (total $Me^{201}Hg$/total ^{201}THg in medium) and SUVA (c) or sulfur content (d). Dashed lines show average $Me^{201}Hg$ production in DOM-free controls. Error bars show standard deviations of triplicate methylation assays and, where not visible, are smaller than the data markers.

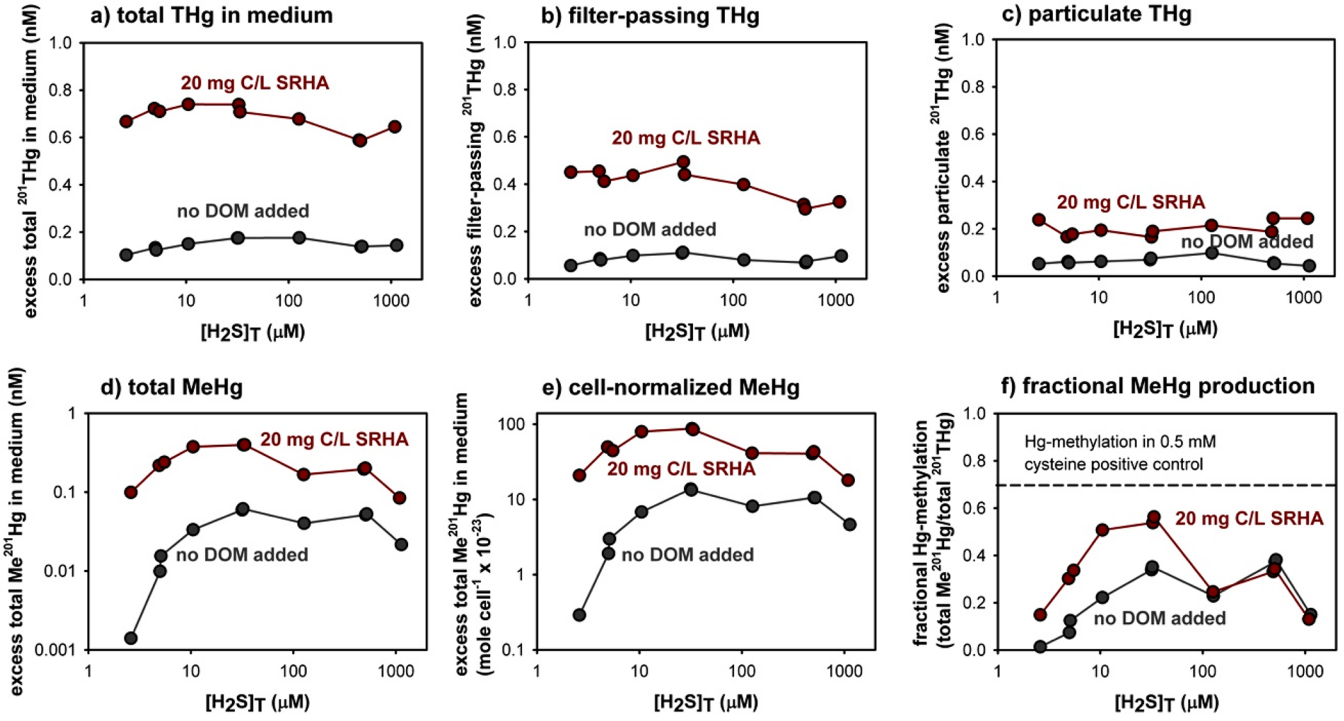

Figure 3. Effect of DOM addition (20 mg C/L Suwannee River humic acid (SRHA)) on Hg methylation by strain ND132 across a sulfide gradient. In these experiments, 1.0 nM $^{201}HgCl_2$ was pre-equilibrated with minimal medium containing either 0 or 20 mg C/L SRHA for 24 h, then spiked with 0 to ~1200 μM Na_2S. The Hg–DOM–S solution was reacted for 2 h prior to introducing the solution to strain ND132. Cells were incubated for 3 h at 31 °C and total ^{201}Hg (^{201}THg) partitioning (a, b, c) and $Me^{201}Hg$ production (d, e, f) were measured at the end of the experiment. Data in d and e are shown on log scale to facilitate comparison. Cell suspension pH values increased from 7.33 to 8.33 as $[H_2S]_T$ increased from 3 to ~1000 μM (pH values tabulated in Table S2 of Supporting Information).

dx.doi.org/10.1021/es400414a | Environ. Sci. Technol. 2013, 47, 5746–5754

with hydrophobic dissolved organic carbon concentration[27] and negatively correlated with spectral slope ratio[28] (spectral slope ratio is inversely correlated with $SUVA_{254}$ and decreases with increasing DOM aromaticity and average molecular weight[46]).

More surprising was our finding that Hg methylation in Hg-DOM-sulfide solutions was correlated with the total S content of the DOM isolates. Under low Hg/DOM ratio conditions, Hg can form complexes with strong thiol binding sites in DOM.[1,2,47] The complexation reaction can be written:

$$Hg^{2+} + 2RS^{-} = Hg(SR)_2 \quad (2)$$

where RS^- is a reduced thiol site in DOM. Strong Hg-binding thiol sites are only a fraction of total DOM sulfur content, but total S content and reduced S content (determined by XANES in a previous study[16]) were strongly correlated for the subset of samples for which reduced S content data were available (r^2 = 0.89, n = 7). While our two-parameter regression model is based upon total DOM S content, it is likely that DOM thiol content is the significant predictor of Hg methylation in DOM−Hg−sulfide solutions. Our previous thermodynamic modeling indicates that, even allowing for a very large binding constant for $Hg(SR)_2$ formation (i.e., log K = 42.0[47]), DOM-thiols will not outcompete inorganic sulfide for $Hg(II)_i$ under common field conditions in anaerobic sediments and saturated soils, that is, when DOM concentrations are on the order of 10s of mg C/L and $[H_2S_T]$ is present at μM concentrations.[18] While DOM thiols are not predicted to be present in sufficient quantity so as to totally solubilize HgS(s), DOM thiols may play an important role in surface adsorption of DOM onto nascent HgS particles, perhaps through interaction with coordinatively unsaturated surface Hg atoms. This idea is analogous to the ternary complex of Hg, DOM, and sulfide proposed by Miller et al.[23] except that DOM thiols would be coordinated to a surface Hg−S species rather than an aqueous species. The apparent independence of S content (or reduced S content) on DOM interaction with metal sulfide particles observed in prior studies[16,24] may be a reflection of the much higher metal/DOM ratios used (e.g., 5 μmol Zn/mg C in Deonarine et al.[24]) compared to this work (0.025 nmol Hg/mg C). At lower Hg/DOM ratios, interactions of specific S-containing DOM functional groups (e.g., thiols, thioethers, organic polysulfides, etc.[48]) with the HgS surface may play a role in slowing HgS nanoparticle/cluster growth, leading to enhanced $Hg(II)_i$ bioavailability. In summary, we hypothesize that both steric and HgS−DOM ligand interactions are important to DOM inhibition of HgS particle growth/aggregation which in turn leads to the demonstrated effect of DOM character on Hg methylation in Hg−DOM−S solutions.

Effect of DOM Across a Sulfide Concentration Gradient. Having demonstrated that DOM concentration[18] and character (this paper) were important drivers of Hg methylation under mildly sulfidic conditions (<10 μM H_2S_T), we set out to ask whether DOM enhanced Hg methylation over a wider range of sulfide concentrations as encountered in natural environments. Figure 3 shows the results of an experiment comparing Hg methylation across a sulfide gradient either with or without 20 mg C/L of SRHA, a strong enhancer of Hg-methylation in low sulfide solutions.

In both the SRHA and DOM-free treatments, significant loss of added $^{201}HgCl_2$ occurred due to sorption of ^{201}Hg onto bottle walls during the 24 pre-equilibration period of Hg with SRHA and medium components (Figure 3a). Sorptive losses were more substantial in the DOM-free treatments, resulting in a total ^{201}Hg pool available for methylation that was ∼5−6 times lower in the DOM-free experiments compared to the experiments with SRHA. Partitioning of ^{201}THg between the filterable and particulate phases was roughly constant over the sulfide concentration gradient for both the DOM-free and SRHA experiments. However, it should be noted that medium pH was almost 1 unit higher at the highest sulfide concentrations due to insufficient buffering capacity upon addition of mM levels of Na_2S to minimal medium containing only 5 mM 3-(N-morpholino)propanesulfonate (MOPS) buffer (see Supporting Information Table S2).

Maximal $Me^{201}Hg$ production, both in the presence and absence of SRHA occurred at a H_2S_T concentration of ∼10−30 μM. Across the entire sulfide gradient, substantially more Hg methylation was observed in the treatments with 20 mg C/L SRHA, with 4−70 times more MeHg produced in the SRHA treatments (Figures 3d and e). In these sulfide gradient experiments, DOM may have enhanced total Hg methylation in part by increasing the total dissolved Hg concentration available for methylation (Figures 3a and b). Because total ^{201}THg in the medium was substantially different in SRHA and DOM-free experiments, examining trends in the percentage of ^{201}THg methylated (total $Me^{201}Hg$/total ^{201}THg in medium) is more instructive (Figure 3f). Comparing $\%Me^{201}Hg$ production, we see that the addition of SRHA only significantly impacts Hg methylation for $[H_2S_T] \leq$ ∼30 μM. The increase in %Hg methylation observed at the lowest sulfide concentration (∼10-fold increase in $\%Me^{201}Hg$) was similar to that observed in separate experiments involving this isolate with similar sulfide, DOC, and ^{201}THg concentrations.[18]

The DOM enhancement factor (defined as the % methylation with DOM relative to % methylation without DOM) decreased substantially with increasing $[H_2S]_T$ for 1 ≤ $[H_2S]_T \leq$ 100 μM (Figure 4). At total sulfide concentrations above 100 μM we observed no difference in Hg-methylation with and without DOM. Our observation that DOM enhances Hg methylation only at low sulfide concentrations (<∼30 μM H_2S_T) is consistent with the idea that DOM enhances Hg-methylation primarily by stabilizing Hg−S clusters or nanoparticles that dominate Hg speciation at relatively low sulfide concentrations. At higher sulfide concentrations, truly dissolved Hg−S complexes ($HgS_xH_y^{(2-2x+y)}$) are expected to become the

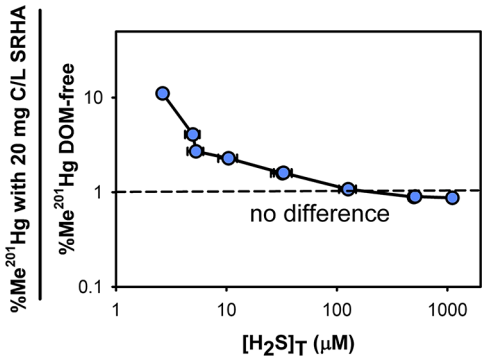

Figure 4. Enhancement in MeHg production by Suwannee River Humic Acid (SRHA) ($\%Me^{201}Hg$ for 20 mg C/L SRHA experiment/$\%Me^{201}Hg$ in DOM-free experiment) vs total sulfide concentration ($[H_2S]_T$). Error bars represent relative percent difference between duplicate treatments, and where not visible are smaller than data markers.

dx.doi.org/10.1021/es400414a | Environ. Sci. Technol. 2013, 47, 5746−5754

dominant Hg−S species at the expense of bulk or nanoscale β-HgS(s) (sample calculations are shown in Supporting Information Table S3). If, as we hypothesize, the primary of role of DOM in enhancing Hg bioreactivity is via particle stabilization and/or growth inhibition, we do not anticipate DOM to appreciably affect bioavailability under conditions thermodynamically unfavorable for β-HgS(s) formation.

The increase in $Hg(II)_i$ bioavailability with increasing $[H_2S]_T$ (up to about 100 μM total sulfide in both DOM-rich and DOM-free solutions) may be indicative of a higher relative bioavailability for truly dissolved HgS species relative to nanoparticulate β-HgS(s).[25] The trend of increasing bioavailability with increasing sulfide concentration was reproducible over a large number of independent washed cell experiments in DOM-free solutions (Figure 5), giving us high confidence in

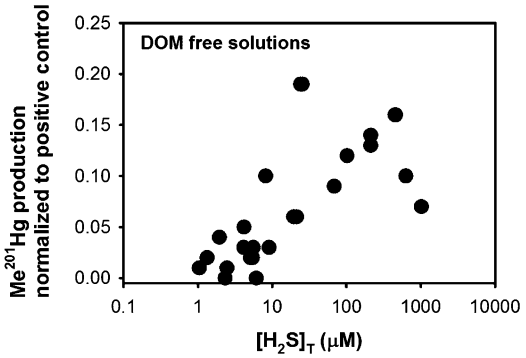

Figure 5. Effect of sulfide concentration on Hg methylation by ND132 in DOM-free washed cell assays. $Me^{201}Hg$ production data are normalized to $Me^{201}Hg$ concentrations for a corresponding positive control containing 0.5 mM L-cysteine at equivalent cell density and growth stage. Total ^{201}Hg concentrations measured at the end of the experiments ranged from 0.12 to 0.37 nM (mean = 0.23 ± 0.08 nM); pH ranged from 7.14 to 8.33 (mean = 7.38 ± 0.28). Note that data corresponding to high sulfide concentrations (>300 μM) had significantly higher pH than the mean (>7.5).

this result. The decrease in %methylation at the highest sulfide concentrations (Figure 4) may be an artifact of a pH shift favoring formation of deprotonated forms of Hg−S (i.e., HgS_2H^- and HgS_2^{2-}) at the expense of neutral $Hg(SH)_2$ (see Supporting Information Table S3), the magnitude of this decrease depending upon the choice of equilibrium constant for β HgS(s) solubility. Previous studies have postulated that $Hg(II)_i$ bioavailability and uptake is controlled by passive diffusion of neutral dissolved Hg species across the cell wall and membrane.[21,22,49,50] At present, we are reluctant to assign the increase in Hg bioavailability with increasing sulfide to a particular species (i.e., neutral Hg−S species) for two reasons. First, and most importantly, numerous studies[12−14,18,25] indicate that equilibrium may not be a relevant concept for Hg−S−DOM systems and hence Hg−S biouptake. Second, even if one were to suppose equilibrium, the large uncertainty associated with log K_{S0} for dissolution of β-HgS(s) (magnified if one considers the potential effects of particle size on the overall thermodynamic driving force[51]), precludes reliable calculations of $Hg(II)_i$ speciation in solutions that are either slightly under- or slightly oversaturated with respect to β-HgS(s). We note that this uncertainty likely applies to predictions of Hg(II) speciation in natural waters or sediment porewaters, where total Hg concentrations are often similar to or lower than those used in the current study (0.1−1 nM).

In many field studies of Hg methylation in sediments and soils, sulfide is a highly significant correlate of Hg methylation or MeHg accumulation. Often, a sulfide concentration at which MeHg production is maximal is observed, and above which MeHg production declines. The optimal sulfide concentration varies significantly among ecosystems, ranging from roughly 1 to 100 μM,[21,28,52−56] although the maxima is most often at or below 10 μM. Our finding of enhanced methylation over a sulfide gradient of 1 to perhaps 100 μM stands in contrast to a number of these previous field and laboratory[50,57] studies reporting inhibition of methylation over this sulfide range. An important distinction of the present report from previous work is the fact that THg concentration and Hg partitioning (measured as filter-passing THg) were essentially invariant over the sulfide gradient studied herein. Significant changes in total Hg concentration and aqueous phase $Hg(II)_i$ concentration may complicate apparent relationships between sulfide concentration and MeHg production. Additionally, in field soils and sediments, sulfide production leads to formation of Hg-reactive particulate phases, namely FeS(s) (mackinawite) and FeS_2 (pyrite), that may alter Hg bioavailability. These complexities are absent from our washed cell laboratory experiments. Importantly, these experiments were done in very short time frames, while natural environments represent longer periods of equilibration. The complexity of the relationships between sulfide, DOM and MeHg production deserves further study, including the kinetics of complex and particle formation, and the applicability of these findings to Hg in mixed metal−sulfide nanoparticles.

Environmental Implications. Observed correlations between DOM concentrations and Hg methylation rates, MeHg concentrations, and sediment-pore water distribution coefficients (K_d) show that DOM is an important control on MeHg fate and transport in sediments and soils.[28,54,58] Our findings here show that DOM character, in addition to concentration, influences MeHg production in nature. DOM size, hydrophobicity, and sulfur content all appear to influence $Hg(II)_i$ bioavailability to Hg-methylating bacteria in the presence of micromolar sulfide concentrations. Our findings provide a rationale for the previous identification of environments with high concentrations or fluxes of highly aromatic DOM—particularly wetlands and upland/wetland interfaces—as MeHg production hot spots.[7,27,28,59] Special consideration to limiting Hg and sulfate deposition to such environments is warranted in order to most effectively limit MeHg production and exposure.

■ ASSOCIATED CONTENT

Supporting Information

Supplemental tables and figure. This material is available free of charge via the Internet at http://pubs.acs.org.

■ AUTHOR INFORMATION

Corresponding Author

*E-mail: grahaman@grinnell.edu; phone: 641-269-9813.

Notes

The authors declare no competing financial interest.

■ ACKNOWLEDGMENTS

We thank A. Bullock, A. Maizel, G. Riedel, Tyler Bell (SERC), K. Butler and B. Poulin (USGS) for laboratory assistance. This paper benefited from the instructive comments of Jeff Jeremiason and three anonymous reviewers. This work was

supported by the U.S. Department of Energy under the Subsurface Biogeochemical Research Program, Office of Science, through the Mercury Science Focus Area Program at Oak Ridge National Laboratory, by U.S. National Science Foundation grant DEB0351050 to A. Heyes and C.C.G., and by the U.S. Geological Survey Priority Ecosystems and Toxics Substances Hydrology Programs. Any use of trade, firm, or product names is for descriptive purposes only and does not imply endorsement by the U.S. government.

REFERENCES

(1) Benoit, J.; Mason, R.; Gilmour, C.; Aiken, G. Constants for mercury binding by dissolved organic matter isolates from the Florida Everglades. *Geochim. Cosmochim. Acta* **2001**, *65*, 4445−4451.

(2) Haitzer, M.; Aiken, G.; Ryan, J. Binding of mercury(II) to dissolved organic matter: The role of the mercury-to-DOM concentration ratio. *Environ. Sci. Technol.* **2002**, *36*, 3564−3570.

(3) Haitzer, M.; Aiken, G.; Ryan, J. Binding of mercury(II) to aquatic humic substances: Influence of pH and source of humic substances. *Environ. Sci. Technol.* **2003**, *37*, 2436−2441.

(4) Lamborg, C.; Tseng, C.; Fitzgerald, W.; Balcom, P.; Hammerschmidt, C. Determination of the mercury complexation characteristics of dissolved organic matter in natural waters with "reducible Hg" titrations. *Environ. Sci. Technol.* **2003**, *37*, 3316−3322.

(5) Han, S.; Gill, G. Determination of mercury complexation in coastal and estuarine waters using competitive ligand exchange method. *Environ. Sci. Technol.* **2005**, *39*, 6607−6615.

(6) Schuster, P. F.; Striegl, R. G.; Aiken, G. R.; Krabbenhoft, D. P.; Dewild, J. F.; Butler, K.; Kamark, B.; Dornblaser, M. Mercury export from the Yukon River Basin and potential response to a changing climate. *Environ. Sci. Technol.* **2011**, *45*, 9262−9267.

(7) Bergamaschi, B. A.; Krabbenhoft, D. P.; Aiken, G. R.; Patino, E.; Rumbold, D. G.; Orem, W. H. Tidally driven export of dissolved organic carbon, total mercury, and methylmercury from a mangrove-dominated estuary. *Environ. Sci. Technol.* **2012**, *46*, 1371−1378.

(8) Khwaja, A. R.; Bloom, P. R.; Brezonik, P. L. Binding strength of methylmercury to aquatic NOM. *Environ. Sci. Technol.* **2010**, *44*, 6151−6156.

(9) Dong, W.; Liang, L.; Brooks, S.; Southworth, G.; Gu, B. Roles of dissolved organic matter in the speciation of mercury and methylmercury in a contaminated ecosystem in Oak Ridge, Tennessee. *Environ. Chem.* **2010**, *7*, 94−102.

(10) Mitchell, C. P. J.; Jordan, T. E.; Heyes, A.; Gilmour, C. C. Tidal exchange of total mercury and methylmercury between a salt marsh and a Chesapeake Bay sub-estuary. *Biogeochemistry* **2012**, *111* (1−3), 583−600.

(11) Ravichandran, M.; Aiken, G.; Ryan, J.; Reddy, M. Inhibition of precipitation and aggregation of metacinnabar (mercuric sulfide) by dissolved organic matter isolated from the Florida Everglades. *Environ. Sci. Technol.* **1999**, *33*, 1418−1423.

(12) Deonarine, A.; Hsu-Kim, H. Precipitation of mercuric sulfide nanoparticles in NOM-containing water: Implications for the natural environment. *Environ. Sci. Technol.* **2009**, *43*, 2368−2373.

(13) Slowey, A. J. Rate of formation and dissolution of mercury sulfide nanoparticles: The dual role of natural organic matter. *Geochim. Cosmochim. Acta* **2010**, *74*, 4693−4708.

(14) Gerbig, C.; Kim, C.; Stegemeier, J.; Ryan, J. N.; Aiken, G. R. Formation of nanocolloidal metacinnabar in mercury-DOM-sulfide systems. *Environ. Sci. Technol.* **2011**, *45*, 9180−9187.

(15) Ravichandran, M.; Aiken, G.; Reddy, M.; Ryan, J. Enhanced dissolution of cinnabar (mercuric sulfide) by dissolved organic matter isolated from the Florida Everglades. *Environ. Sci. Technol.* **1998**, *32*, 3305−3311.

(16) Waples, J.; Nagy, K.; Aiken, G.; Ryan, J. Dissolution of cinnabar (HgS) in the presence of natural organic matter. *Geochim. Cosmochim. Acta* **2005**, *69*, 1575−1588.

(17) Barkay, T.; Gillman, M.; Turner, R. Effects of dissolved organic carbon and salinity on bioavailability of mercury. *Appl. Environ. Microb.* **1997**, *63*, 4267−4271.

(18) Graham, A. M.; Aiken, G. R.; Gilmour, C. C. Dissolved organic matter enhances microbial mercury methylation under sulfidic conditions. *Environ. Sci. Technol.* **2012**, *46*, 2715−2723.

(19) Compeau, G. C.; Bartha, R. Sulfate-reducing bacteria - principal methylators of mercury in anoxic estuarine sediment. *Appl. Environ. Microb.* **1985**, *50*, 498−502.

(20) Gilmour, C. C.; Henry, E. A.; Mitchell, R. Sulfate stimulation of mercury methylation in freshwater sediments. *Environ. Sci. Technol.* **1992**, *26*, 2281−2287.

(21) Drott, A.; Lambertsson, L.; Bjorn, E.; Skyllberg, U. Importance of dissolved neutral mercury sulfides for methyl mercury production in contaminated sediments. *Environ. Sci. Technol.* **2007**, *41*, 2270−2276.

(22) Benoit, J.; Gilmour, C.; Mason, R.; Heyes, A. Sulfide controls on mercury speciation and bioavailability to methylating bacteria in sediment pore waters. *Environ. Sci. Technol.* **1999**, *33*, 951−957.

(23) Miller, C. L.; Mason, R. P.; Gilmour, C. C.; Heyes, A. Influence of dissolved organic matter on the complexation of mercury under sulfidic conditions. *Environ. Toxicol. Chem.* **2007**, *26*, 624−633.

(24) Deonarine, A.; Lau, B. L. T.; Aiken, G.; Ryan, J.; Hsu-Kim, H. Effects of humic substances on precipitation and aggregation of zinc sulfide nanoparticles. *Environ. Sci. Technol.* **2011**, *45*, 3217−3223.

(25) Zhang, T.; Kim, B.; Levard, C.; Reinsch, B. C.; Lowry, G. V.; Deshusses, M. A.; Hsu-Kim, H. Methylation of mercury by bacteria exposed to dissolved, nanoparticulate, and microparticulate mercuric sulfides. *Environ. Sci. Technol.* **2012**, *46*, 6950−6958.

(26) Weishaar, J. L.; Aiken, G. R.; Bergamaschi, B. A.; Fram, M. S.; Fujii, R.; Mopper, K. Evaluation of specific ultraviolet absorbance as an indicator of the chemical composition and reactivity of dissolved organic carbon. *Environ. Sci. Technol.* **2003**, *37*, 4702−4708.

(27) Hall, B. D.; Aiken, G. R.; Krabbenhoft, D. P.; Marvin-Dipasquale, M.; Swarzenski, C. M. Wetlands as principal zones of methylmercury production in southern Louisiana and the Gulf of Mexico region. *Environ. Pollut.* **2008**, *154*, 124−134.

(28) Mitchell, C. P. J.; Gilmour, C. C. Methylmercury production in a Chesapeake Bay salt marsh. *J. Geophys. Res.-Biogeo.* **2008**, *113*, G00C04.

(29) Gerbig, C. The effects of dissolved organic matter on mercury-sulfide interactions in aqueous systems, Ph.D. Dissertation, University of Colorado, 2011.

(30) Dittman, J. A.; Shanley, J. B.; Driscoll, C. T.; Aiken, G. R.; Chalmers, A. T.; Towse, J. E.; Selvendiran, P. Mercury dynamics in relation to dissolved organic carbon concentration and quality during high flow events in three northeastern U.S. streams. *Water Resour. Res.* **2010**, *46*, W07522.

(31) Aiken, G. R.; Gilmour, C. C.; Krabbenhoft, D. P.; Orem, W. Dissolved organic matter in the Florida Everglades: implications for ecosystem restoration. *Crit. Rev. Environ. Sci. Technol.* **2011**, *41*, 217−248.

(32) Haaland, S.; Hongve, D.; Laudon, H.; Riise, G.; Vogt, R. D. Quantifying the drivers of the increasing colored organic matter in boreal surface waters. *Environ. Sci. Technol.* **2010**, *44*, 2975−2980.

(33) SanClements, M. D.; Oelsner, G. P.; McKnight, D. M.; Stoddard, J. L.; Nelson, S. J. New insights into the source of decadal increases of dissolved organic matter in acid-sensitive lakes of the northeastern United States. *Environ. Sci. Technol.* **2012**, *46*, 3212−3219.

(34) Thurman, E. M.; Malcolm, R. L. Preparative isolation of aquatic humic substances. *Environ. Sci. Technol.* **1981**, *15*, 463−466.

(35) Aiken, G.; McKnight, D.; Thorn, K. A.; Thurman, E. M. Isolation of hydrophilic organic-acids from water using nonionic macroporous resins. *Org. Geochem.* **1992**, *18*, 567−573.

(36) Gilmour, C. C.; Tuttle, J. H.; Means, J. C. Anaerobic microbial methylation of inorganic tin in estuarine sediment slurries. *Microb. Ecol.* **1987**, *14*, 233−242.

(37) Gilmour, C. C.; Elias, D. A.; Kucken, A. M.; Brown, S. D.; Palumbo, A. V.; Schadt, C. W.; Wall, J. D. Sulfate-reducing bacterium

Desulfovibrio desulfuricans ND132 as a model for understanding bacterial mercury methylation. *Appl. Environ. Microb.* **2011**, *77*, 3938−3951.
(38) Graham, A. M.; Bullock, A. L.; Maizel, A. C.; Elias, D. A.; Gilmour, C. C. A Detailed assessment of the kinetics of Hg-cell association, Hg methylation, and MeHg degradation in several *Desulfovibrio* species. *Appl. Environ. Microb.* **2012**, *78*, 7337−7346.
(39) Brown, S. D.; Gilmour, C. C.; Kucken, A. M.; Wall, J. D.; Elias, D. A.; Brandt, C. C.; Podar, M.; Chertkov, O.; Held, B.; Bruce, D. C.; Detter, J. C.; Tapia, R.; Han, C. S.; Goodwin, L. A.; Cheng, J.-F.; Pitluck, S.; Woyke, T.; Mikhailova, N.; Ivanova, N. N.; Han, J.; Lucas, S.; Lapidus, A. L.; Land, M. L.; Hauser, L. J.; Palumbo, A. V. Genome sequence of the mercury-methylating strain *Desulfovibrio desulfuricans* ND132. *J. Bacteriol.* **2011**, *193*, 2078−2079.
(40) Schaefer, J. K.; Rocks, S. S.; Zheng, W.; Liang, L.; Gu, B.; Morel, F. M. M. Active transport, substrate specificity, and methylation of Hg(II) in anaerobic bacteria. *Proc. Natl. Acad. Sci. U.S.A.* **2011**, *108*, 8714−8719.
(41) Clesceri, L. S., Greenberg, A. E., Eaton, A. D, Eds. *Standard Methods for the Examination of Water and Wastewater*; American Public Health Association: Washington, D.C., 2000.
(42) Bradford, M. M. Rapid and sensitive method for quantitation of microgram quantities of protein utilizing principle of protein-dye binding. *Anal. Biochem.* **1976**, *72*, 248−254.
(43) Hintelmann, H.; Ogrinc, N. Determination of stable mercury isotopes by ICP/MS and their application in environmental studies. In *Biogeochemistry of Environmentally Important Trace Metals*; Cai, Y., Braids, C. O., Eds.; American Chemical Society: Washington, D.C., 2003; pp 321−338.
(44) Bancon-Montigny, C.; Yang, L.; Sturgeon, R. E.; Colombini, V.; Mester, Z. High-yield synthesis of milligram amounts of isotopically enriched methylmercury($CH_3{}^{198}HgCl$). *Appl. Organomet. Chem.* **2004**, *18*, 57−64.
(45) Schaefer, J. K.; Morel, F. M. M. High methylation rates of mercury bound to cysteine by *Geobacter sulfurreducens*. *Nat. Geosci.* **2009**, *2*, 123−126.
(46) Helms, J. R.; Stubbins, A.; Ritchie, J. D.; Minor, E. C.; Kieber, D. J.; Mopper, K. Absorption spectral slopes and slope ratios as indicators of molecular weight, source, and photobleaching of chromophoric dissolved organic matter. *Limnol. Oceanogr.* **2008**, *53*, 955−969.
(47) Skyllberg, U. Competition among thiols and inorganic sulfides and polysulfides for Hg and MeHg in wetland soils and sediments under suboxic conditions: Illumination of controversies and implications for MeHg net production. *J. Geophys. Res.-Biogeo.* **2008**, *113*, G00C03.
(48) Vairavamurthy, M.; Maletic, D.; Wang, S.; Manowitz, B.; Eglinton, T.; Lyons, T. Characterization of sulfur-containing functional groups in sedimentary humic substances by X-ray absorption near-edge structure spectroscopy. *Energy Fuels* **1997**, *11*, 546−553.
(49) Mason, R.; Reinfelder, J.; Morel, F. Uptake, toxicity, and trophic transfer of mercury in a coastal diatom. *Environ. Sci. Technol.* **1996**, *30*, 1835−1845.
(50) Benoit, J.; Gilmour, C.; Mason, R. Aspects of bioavailability of mercury for methylation in pure cultures of Desulfobulbus propionicus (1pr3). *Appl. Environ. Microb.* **2001**, *67*, 51−58.
(51) Navrotsky, A.; Mazeina, L.; Majzlan, J. Size-driven structural and thermodynamic complexity in iron oxides. *Science* **2008**, *319*, 1635−1638.
(52) Gilmour, C.; Riedel, G.; Ederington, M.; Bell, J.; Benoit, J.; Gill, G.; Stordal, M. Methylmercury concentrations and production rates across a trophic gradient in the northern Everglades. *Biogeochemistry* **1998**, *40*, 327−345.
(53) Hollweg, T. A.; Gilmour, C. C.; Mason, R. P. Methylmercury production in sediments of Chesapeake Bay and the mid-Atlantic continental margin. *Mar. Chem.* **2009**, *114*, 86−101.
(54) Hollweg, T. A.; Gilmour, C. C.; Mason, R. P. Mercury and methylmercury cycling in sediments of the mid-Atlantic continental shelf and slope. *Limnol. Oceanogr.* **2010**, *55*, 2703−2722.
(55) Hammerschmidt, C.; Fitzgerald, W. Geochemical controls on the production and distribution of methylmercury in near-shore marine sediments. *Environ. Sci. Technol.* **2004**, *38*, 1487−1495.
(56) Hammerschmidt, C. R.; Fitzgerald, W. F.; Balcom, P. H.; Visscher, P. T. Organic matter and sulfide inhibit methylmercury production in sediments of New York/New Jersey Harbor. *Mar. Chem.* **2008**, *109*, 165−182.
(57) Benoit, J.; Gilmour, C.; Mason, R. The influence of sulfide on solid phase mercury bioavailability for methylation by pure cultures of *Desulfobulbus propionicus* (1pr3). *Environ. Sci. Technol.* **2001**, *35*, 127−132.
(58) Marvin-DiPasquale, M.; Lutz, M. A.; Brigham, M. E.; Krabbenhoft, D. P.; Aiken, G. R.; Orem, W. H.; Hall, B. D. Mercury cycling in stream ecosystems. 2. Benthic methylmercury production and bed sediment−pore water partitioning. *Environ. Sci. Technol.* **2009**, *43*, 2726−2732.
(59) Mitchell, C. P. J.; Branfireun, B. A.; Kolka, R. K. Spatial characteristics of net methylmercury production hot spots in peatlands. *Environ. Sci. Technol.* **2008**, *42*, 1010−1016.

Supporting Information
to

Effect of Dissolved Organic Matter Source and Character on Microbial Hg Methylation in Hg-S-DOM Solutions

Andrew M. Graham,[1,2*] George R. Aiken[3] and Cynthia C. Gilmour[2]

[1]Grinnell College Department of Chemistry, Noyce Science Center, 1116 8th Avenue, Grinnell IA 50112-1690, United States
[2]Smithsonian Environmental Research Center, 647 Contees Wharf Rd, Edgewater MD 21037, United States
[3]U.S. Geological Survey, 3215 Marine Street, Suite E127, Boulder, Colorado 80303, United States
[*]Corresponding Author
email: grahaman@grinnell.edu
phone: 641-269-9813

Contents

7 pages total

Table S1. Ancillary data for Hg methylation assays with various DOM isolates. Experiments were run in two batches (a and b) on different days with separate controls (no DOM and no DOM with 500 µM L-cysteine) for each batch. Batch "a" is indicated by light gray, and batch "b" in darker gray. For cell density, cell-protein, and pH, reported quantities are the average of 3 replicates at t=0 h and t=3 h. Error estimates are standard deviations of triplicate methylation assays.

Treatment	Cell density (x 10^8 cells/mL)	Total cell protein (mg/L)	pH	Initial $[H_2S]_T$ (µM)	Final (t=3h) $[H_2S]_T$ (µM)	Total $Me^{201}Hg$ production in 3 h (pM)
No DOM control (a)	7.81±0.26	48.4±0.7	7.59±0.01	1.54±0.09	1.33±0.09	5.90±0.10
No DOM + 500 M L-cys control (a)	8.01±0.19	48.4±1.4	7.32±0.01	4.27±0.03	22.62±0.32	260±5
20 mg C/L 2BSHPoA	5.68±0.54	33.1±2.5	7.48±0.02	1.35±0.01	1.37±0.05	41.8±1.3
20 mg C/L F1HPoA	5.75±0.14	37.4±0.8	7.47±0.01	1.30±0.12	1.34±0.01	99.2±2.8
20 mg C/L F1TPiA	5.83±0.61	36.5±2.0	7.47±0.01	1.64±0.04	1.52±0.13	36.6±0.4
20 mg C/L SRHA	5.81±0.13	40.8±0.4	7.47±0.02	1.43±0.06	1.58±0.08	45.4±0.5
20 mg C/L WLHPoA	8.01±0.34	49.2±1.1	7.47±0.01	1.63±0.13	1.52±0.03	11.0±0.1
20 mg C/L WLTPiA	7.92±0.22	47.2±1.1	7.48±0.01	2.11±0.03	1.95±0.06	10.6±0.2
NO DOM control (b)	7.32±0.19	49.6±8.0	7.37±0.01	1.32±0.11	1.04±0.08	2.18±0.05
No DOM + 500 M L-cys control (b)	7.16±0.21	45.7±1.9	7.30±0.02	3.33±0.12	17.61±0.47	219±5
20 mg C/L MRFA	6.21±0.34	39.1±0.9	7.31±0.01	0.97±0.11	1.30±0.03	5.37±0.13
20 mg C/L OgRFA	6.22±0.34	39.1±3.7	7.31±0.01	1.18±0.05	1.26±0.07	32.1±2.1
20 mg C/L OhRFA	6.31±0.12	37.7±1.4	7.30±0.02	1.39±0.05	1.54±0.01	21.2±0.6
20 mg C/L POFA	5.96±0.23	40.4±1.3	7.33±0.01	1.25±0.04	1.25±0.05	5.21±0.11
20 mg C/L PRHPoA	6.99±0.13	46.5±1.7	7.33±0.01	1.42±0.12	1.33±0.02	19.3±0.4
20 mg C/L PRTPiA	7.34±0.10	45.4±1.2	7.33±0.01	2.17±0.03	1.89±0.02	10.4±0.1

Table S2. Summary of ancillary data for sulfide gradient experiment with Suwannee River humic acid (SRHA). Data in light gray are for experiments without added DOM, data in dark gray are for experiments with 20 mg C/L SRHA, data in white are for positive controls without sulfide amendment but with 500 µM L-cysteine. Treatment relative percent differences (RPDs) were 5.4±6.7% for cell density, 0.19±0.14% for pH, and 4.0±4.8% for sulfide.

Treatment	Cell density (x 10^8 cells/mL)	pH	Initial $[H_2S]_T$ (µM)	Final (t=3h) $[H_2S]_T$ (µM)
No DOM, no sulfide spike	4.78	7.33	3.0	2.3
No DOM, sulfide spike 1	5.22	7.32	5.9	4.1
No DOM, sulfide spike 1 replicate	5.19	7.34	6.0	4.2
No DOM, sulfide spike 2	4.90	7.33	12.8	8.2
No DOM, sulfide spike 3	4.32	7.36	39.4	24.0
No DOM, sulfide spike 3 replicate	4.60	7.37	39.1	25.4
No DOM, sulfide spike 4	4.96	7.48	152.7	101.8
No DOM, sulfide spike 5	4.86	7.81	568.2	449.1
No DOM, sulfide spike 5 replicate	5.02	7.84	577.5	460.1
No DOM, sulfide spike 6	4.66	8.33	1248.1	1019.0
20 mg C/L SRHA, no sulfide spike	4.75	7.3	2.7	2.6
20 mg C/L SRHA, sulfide spike 1	4.39	7.3	4.9	4.9
20 mg C/L SRHA, sulfide spike 1 replicate	5.37	7.31	5.9	5.1
20 mg C/L SRHA, sulfide spike 2	4.71	7.31	11.4	9.5
20 mg C/L SRHA, sulfide spike 3	4.55	7.34	36.0	29.2
20 mg C/L SRHA, sulfide spike 3 replicate	4.69	7.34	36.0	30.9
20 mg C/L SRHA, sulfide spike 4	4.04	7.42	135.2	116.8
20 mg C/L SRHA, sulfide spike 5	4.81	7.76	499.0	475.3
20 mg C/L SRHA, sulfide spike 5 replicate	4.67	7.79	511.3	495.0
20 mg C/L SRHA, sulfide spike 6	4.68	8.28	1052.6	1123.2
No DOM + 500 µM L-cysteine	4.46	7.24	3.6	18.5
No DOM + 500 µM L-cysteine replicate	4.54	7.24	3.5	17.8

Table S3. MINEQL+ (v. 4.5) calculated equilibrium speciation of Hg in DOM-free sulfide gradient experiments (Figure 3 in main paper). Whether β-HgS(s) (metacinnabar) precipitation is predicted at higher sulfide concentrations is dependent upon the choice of log K_{S0} for metacinnabar. All thermodynamic data used for calculation is equivalent to that used in Graham *et al.* (ref 18 in main text).

a) log K_{S0} = 38.0 ($HgS + H^{+} = Hg^{2+} + HS^{-}$)

measured quantities			**modeled equilibrium concentration (M)**					
measured UNF THg (M)	**measured $[H_2S]_T$ (μM)**	**measured pH**	**$Hg(SH)_2$ (aq)**	**HgS_2H^-**	**HgS_2^{2-}**	**HgS(aq)**	**$HgSH^+$**	**metacinnabar**
1.03E-10	2.64	7.33	3.31E-14	6.16E-13	3.06E-13	3.05E-12	9.82E-16	9.90E-11
1.34E-10	5.04	7.32	6.44E-14	1.17E-12	5.67E-13	3.05E-12	1.00E-15	1.29E-10
1.24E-10	5.08	7.34	6.28E-14	1.19E-12	6.06E-13	3.05E-12	9.60E-16	1.19E-10
1.50E-10	10.5	7.33	1.32E-13	2.45E-12	1.22E-12	3.05E-12	9.82E-16	1.43E-10
1.75E-10	31.7	7.36	3.78E-13	7.52E-12	4.00E-12	3.05E-12	9.16E-16	1.60E-10
1.75E-10	32.2	7.37	3.78E-13	7.69E-12	4.19E-12	3.05E-12	8.95E-16	1.60E-10
1.76E-10	127	7.48	1.23E-12	3.21E-11	2.25E-11	3.05E-12	6.95E-16	1.17E-10
1.38E-10	509	7.81	9.70E-13	5.43E-11	8.15E-11	1.15E-12	1.23E-16	undersaturated
1.39E-10	519	7.84	8.75E-13	5.25E-11	8.45E-11	1.08E-12	1.08E-16	undersaturated
1.44E-10	1130	8.33	1.30E-13	2.41E-11	1.20E-10	2.11E-13	6.83E-18	undersaturated

b) **a)** log K_{sp} = 36.0 ($HgS + H^{+} = Hg^{2+} + HS^{-}$)

measured quantities			**modeled equilibrium concentration (M)**					
measured UNF THg (nM)	**measured $[H_2S]_T$ (µM)**	**measured pH**	**$Hg(SH)_2$ (aq)**	**HgS_2H^-**	**HgS_2^{2-}**	**HgS(aq)**	**$HgSH^+$**	**metacinnabar**
1.03E-10	2.64	7.33	8.54E-13	1.58E-11	7.87E-12	7.84E-11	2.53E-14	undersaturated
1.34E-10	5.04	7.32	1.78E-12	3.23E-11	1.57E-11	8.42E-11	2.78E-14	undersaturated
1.24E-10	5.08	7.34	1.59E-12	3.01E-11	1.53E-11	7.70E-11	2.42E-14	undersaturated
1.50E-10	10.5	7.33	2.89E-12	5.36E-11	2.66E-11	6.69E-11	2.16E-14	undersaturated
1.75E-10	31.7	7.36	4.43E-12	8.81E-11	4.69E-11	3.56E-11	1.07E-14	undersaturated
1.75E-10	32.2	7.37	4.32E-12	8.79E-11	4.79E-11	3.48E-11	1.02E-14	undersaturated
1.76E-10	127	7.48	3.66E-12	9.59E-11	6.73E-11	9.09E-12	2.08E-15	undersaturated
1.38E-10	509	7.81	9.70E-13	5.43E-11	8.15E-11	1.15E-12	1.23E-16	undersaturated
1.39E-10	519	7.84	8.75E-13	5.25E-11	8.45E-11	1.08E-12	1.08E-16	undersaturated
1.44E-10	1130	8.33	1.30E-13	2.41E-11	1.20E-10	2.11E-13	6.83E-18	undersaturated

Table S4. Summary of analytical precision, reproducibility and detection limits for total Hg (THg) and methylmercury (MeHg) analyses.

Analysis	**Method**	**Detection Limit[a]**	**RPD[b] of duplicate analyses**	**Spike Recovery**	**SRM[c] recovery**
Total and filter-passing MeHg	Distillation, ethylation, ID-GC-ICP-MS[d]	Tracer[e] MeHg = 2.2 pM; ambient MeHg = 15 pM[f]	1.1±1.1% (*n* = 5 pairs)	n.d.[g]	119.9±14.9% (*n* = 9)[h]
Total and filter-passing THg	HNO_3/H_2SO_4 digestion, flow-injection ICP-MS	Tracer THg = 1.2 pM; ambient THg = 20.6 pM	3.0±3.5% (*n* = 19 pairs)	94.6±6.3% (*n* = 16)	n.d.

[a]Instrument detection limits calculated as 3 times the standard deviation of distillation or digestion blanks. Reported detection limits are method detection limits and account for sample dilution.
[b] Relative percent difference
[c] Standard reference material
[d] ID-GC-ICP-MS = isotope dilution-gas chromatography-inductively coupled plasma-mass spectrometry
[e]Tracer = stable isotope enriched ^{201}Hg
[f]Detection limit calculated for 1 mL sample distillations
[g]n.d. = not detemined
[h]Average recovery of MeHg in oyster tissue SRM (NIST 1566b).

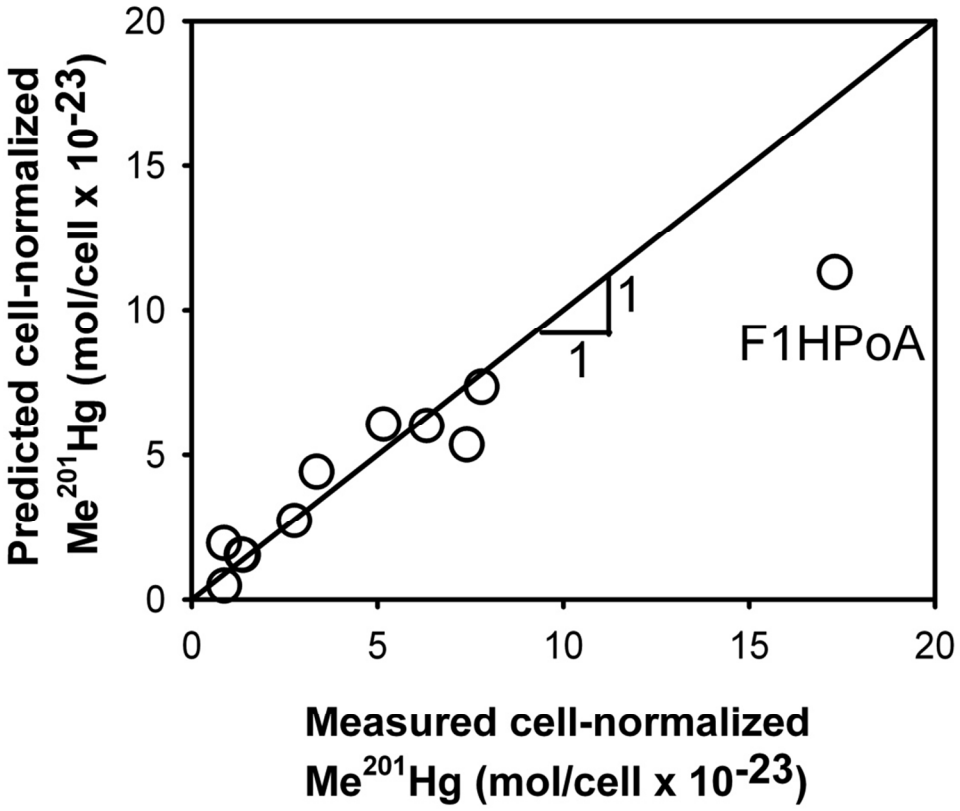

Figure S1. Measured vs. predicted cell-normalized $Me^{201}Hg$ in experiments containing 20 mg C/L DOM isolate, 1.48±0.23 μM $[H_2S]_T$ and 0.32±0.07 nM total ^{201}Hg in the medium. Predictions were based on a linear model including DOM $SUVA_{254}$ and sulfur content as the only explanatory variables. Florida Everglades isolate F1HPoA is noted for deviating significantly from the model.